First-principles calculation of core-level binding energy shift in surface chemical processes

ZENG ZhenHua, MA XiuFang, DING WuChen & LI WeiXue[*]

State Key Laboratory of Catalysis and Center for Theoretical and Computational Chemistry; Dalian Institute of Chemical Physics, Chinese Academy of Sciences, Dalian 116023, China

Combined with third generation synchrotron radiation light sources, X-ray photoelectron spectroscopy (XPS) with higher energy resolution, brilliance, enhanced surface sensitivity and photoemission cross section in real time found extensive applications in solid-gas interface chemistry. This paper reports the calculation of the core-level binding energy shifts (CLS) using the first-principles density functional theory. The interplay between the CLS calculations and XPS measurements to uncover the structures, adsorption sites and chemical reactions in complex surface chemical processes are highlight. Its application on clean low index (111) and vicinal transition metal surfaces, molecular adsorption in terms of sites and configuration, and reaction kinetics are domonstrated.

first principles, core-level binding energy shift, surface chemical processes

1   Introduction

Identification of adsorption sites, structures and chemical states as well as their evolutions on solid surfaces is crucial for understanding the mechanism of surface chemical processes and catalytic reactions at the microscopic level. Among them, core-level photoelectron spectroscopy excited by X-ray (XPS), which is typically operated under ultrahigh vacuum conditions and requires considerable acquisition time for model systems, is one of the most extensively used spectroscopes due to its high surface sensitivity and ability to probe the electronic and geometric structures of solid surfaces with adsorbed molecules [1, 2]. Because of the third generation synchrotron radiation light sources with higher energy resolution, brilliance, enhanced surface sensitivity and photoemission cross section, the scope of XPS has been significantly extended [3, 4]. Particularly, a new class of high pressure and fast XPS allows studies of the kinetics of surface reactions on nano-structural materials under realistic conditions, which is one of the key issues to bridge "pressure-gap" and "materials-gap" from model systems to real catalysts [5]. The latest developments and applications of XPS measurements are available in the comprehensive review of refs. [3, 4] and references therein.

Theoretical calculations of the core-level binding energies and their relative shifts (CLS), using the first-principles density functional theory (DFT), increased considerably in the last two decades for its improvement in accuracy, predictability and ability to uncover the microscopic details of the various surface chemical processes. The applications range from clean surfaces of transition metals (TM) [6–9] and surfaces or interfaces of semiconductors [10–13] to atom/molecule adsorptions on TM surfaces [14–20]. It has been applied to highly under-coordinated surface atoms [21, 22] and the chemical reaction on the surface [23–25]. CLS calculations are also widely used in free molecules in gas phase [26, 27] and alloys [28]. This paper highlights the significance of CLS calculations and the interplay with respect to XPS measurements for deep understanding of the chemical processes on transition metal (TM) surfaces, as

*Corresponding author (email: wxli@dicp.ac.cn)

described below.

One of the advantages of the CLS calculations is its atomic resolved feature, in contrast to the spatial average from XPS measurements. The CLS calculations cooperating with experiments provide a conclusive assignment of XPS spectra [15]. In addition, atomic resolved CLS calculations facilitate the assignment of new peaks for molecular adsorption on defected/corrugated surfaces/nanoparticles, where a number of highly active sites with different coordinations are present and hard to distinguish from the experiments alone [23]. The sensitivity of CLS to the local environments helps the screening of structures via DFT calculations, in which a thorough exploring of the phase space might be computationally demanding and even formidable [29, 30]. Last but not least, for the system with flat potential energy surface, and/or the system which couldnot be properly described by ground state DFT calculations due to the lack of the accurate exchange-correlation functional, distinct CLS may exist and be calculated reliably. This comparison between calculated and measured CLS would provide valuable insights, which cannot be obtained from energetics calculations otherwise [16, 17, 23].

According to Weinert and Watson [31], several effects contribute to the CLSs: interatomic and intra-atomic charge transfer, changes in the screening of the final state of the core-hole and in the Fermi-level relative to the center of gravity of bands, and redistribution of charge due to bonding and hybridization. A reliable theory needs to take all these effects into account. An apparent zero shift observed in experiments does not necessarily imply that the environments of the examined and referenced atoms are the same, and the cancellation of the different effects is possible. These effects could theoretically be distinguished partially using the initial state (IS) approximation by examining the system before excitation of the interested core electrons, and the final state (FS) approximation in the presence of the core-hole, in which the screening effects due to the excitation of the core electrons are included. Depending on the local environments, the screening effect of inequivalent atoms could be different and distinguished by the theoretical calculations, but not accessible by XPS measurements alone. The difference between IS and FS calculations as well as their dependence on the local environments provide valuable insights about the electronic properties of interested atoms [14, 15]. For surface reactions, complex screening processes mediated with the substrates may result in the CLS overlaping of interested atoms in different intermediates [25]. In this case, additional calculations and characterizations are required.

2 Methodology for CLS calculations

Core-level binding energy shifts (E_{CLS}) are the changes of specific core electron binding energies (BE) of interested

atoms and reference atoms, which are typically located in different environments, i.e.,

$$E_{CLS} = BE - BE^{ref} \qquad (1)$$

where BE is defined as the energy required to remove this electron from the interested atoms. To calculate reliable CLS, it is crucial to calculate accurate BE. Depending on the implementations, the initial state (IS) and final state (FS) approximation have been developed. For the IS approximation, core level binding energies are the negative eigenvalue of the specific core orbital before the excitation of one electron in this orbital, i.e.,

$$BE_i^{IS} = -\varepsilon_i^{IS} \qquad (2)$$

The IS approximation leaves out the fact of the possible relaxation and screening after the excitation of the core electron i of the interested atoms, which typically underestimates the BE. Taking the relaxation/screening into account by the FS approximation, the binding energies are calculated by the difference between two separated total energy calculations,

$$BE_i^{FS} = E(n_i - 1) - E(n_i) \qquad (3)$$

where $E(n_i - 1)$ is the total energy of excited system with one electron removing from the specific core orbital to the valence regime (for TM surfaces), and $E(n_i)$ is the total energy of the ground state. In this context, the total energy of the excited system is obtained via minimization of electronic configuration in the presence of the core-hole, and the electron relaxation (FS effect) is included, correspondingly.

To utilize the eigenvalue from DFT calculations and the FS effects, transition state (TS) theory [32] and generalized transition state theory (GTS) [33] were proposed. In GTS theory, a fractional electron x is excited, and the corresponding total energy $E(n_i - x)$ is expanded as a Taylor series:

$$E(q_i = n_i - x) = E(n_i) + \lambda_1 x + \lambda_2 x^2 + \cdots + \lambda_m x^m + \cdots \qquad (4)$$

where $\lambda_m = (-1)^m E^{(m)}(n_i) / m!$

From Janak's theorem [34] we obtained

$$\varepsilon_i = \partial E / \partial n_i \qquad (5)$$

From eqs. (4) and (5), we obtained

$$F(x) = -\varepsilon_i(x) = \lambda_1 + 2\lambda_2 x + \cdots + m\lambda_m x^{m-1} + \cdots \qquad (6)$$

For the TS theory, where half electron is removed from the core to the valence band, the corresponding binding energy is,

$$BE_i^{TS} = F(0.5) = \lambda_1 + \lambda_2 + \frac{3}{4}\lambda_3 \cdots + \frac{m}{2^{m-1}}\lambda_m + \cdots \qquad (7)$$

with an error bar

$$\delta^{\mathrm{TS}} = \frac{1}{4}\lambda_3 + \cdots + \frac{2^{m-1}-m}{2^{m-1}}\lambda_m + \cdots \qquad (8)$$

The binding energy for the GTS theory is,

$$BE_i^{\mathrm{GTS}}$$

$$= \frac{1}{4}F(0) + \frac{3}{4}F\left(\frac{2}{3}\right) = \lambda_1 + \lambda_2 + \lambda_3 + \frac{8}{9}\lambda_4 \cdots + \frac{m}{2}\left(\frac{2}{3}\right)^{m-1}\lambda_m + \cdots$$
$$(9)$$

with an error bar

$$\delta^{\mathrm{GTS}} = \frac{1}{9}\lambda_4 + \cdots + \left(1 - \frac{m}{2}\left(\frac{2}{3}\right)^{m-1}\right)\lambda_m + \cdots \qquad (10)$$

Concerning IS and GTS approximation (including the FS effects), we noticed that they are applicable only when the core-electrons are treated explicitly in the implementation of the total energy calculations, such as all electron density functional theory method and *ab initio* method, but not for pseudopotential (PP) method. The FS approximation calculated by the total energy difference is however applicable for all different implementations, even for PP method if an effective PP with proper excitation of the core electrons is provided, as discussed below. Because the calculation of absolute *BE* remains suffering various approximations and would have considerable error bar, the relative shifts are more reliable due to the error cancellations, and meaningful for the comparison with experiments.

There are various total energy calculation packages with different implementations and approximations, such as the PP method, all electron-like projector augmented wave (PAW) method and full potential linearized augmented plane wave (FP-LAPW) method. Though all of them are able to calculate the CLS including the FS effects, the differences in the calculation procedures and extent of the FS effects included are summarized as follows:

(1) For the PP method, there is no core electron treated explicitly during the total energy calculations, and the effect of the core electron is represented by an effective potential, which is denoted as frozen core (FC) approximation. To simulate the effect of the core-hole, an excited effective PP is generated by removing a specific core electron. To calculate $E(n_i - 1)$, the PP of the interested atoms is replaced by the excited PP. In this framework (under the constraint of the FC approximation), the FS effects from both valence electron and core electron relaxation are included [16, 20].

(2) For the PAW method with all electron-like accuracy and PP-like computational efficiency, the description of the FS effects is improved [17]. The extension of the PAW method beyond the FC approximation by allowing core relaxation explicitly was developed. This significantly improves the overall accuracy and transferability of the CLS calculations [35]. The FS effects have been described more reliably with the explicit core-hole relaxation. In this context, it is noteworthy that even within the FC approximation,

the main FS effects from the core-hole relaxation could be included if excited PAW potential is generated, as in the PP method [35].

(3) The FP-LAPW method treats the core and valence electrons explicitly and is computationally demanding. It describes the complete FS effects from electron and core relaxation, and is regarded as the benchmark to various CLS calculation methods [14, 15, 36]. Its accuracy and explicit treatment of the core electrons self-consistently allow explicit calculation of the absolute *BE*, which could be compared with directly measured core-electron binding energies (see Appendix).

3   CLS for clean vicinal Rh(553)

To demonstrate the sensitivity of CLS with respect to the local environments and accuracy achieved by DFT calculations, we present here a study of clean vicinal Rh(553) surface, which is formed by a (111) terrace with the width of five atoms, separated by monoatomic (111) facet, as plotted in Figure 1(a) and (b). Compared to the bulk atoms with coordination twelve, there are three types of surface atoms with different coordination: 3/5 of the atoms have coordination nine and are on the (111) terraces, 1/5 of the atoms have coordination number seven at the step edges, and the last 1/5 have coordination number eleven underneath the step edges.

By using the high resolution light source, Anderson *et al.* measured Rh $3d_{5/2}$ core level spectrum of the Rh(553) surface [37]. The spectrum was decomposed into four components: beside the bulk peak at higher binding energy, two additional spectra were attributed to the atoms in the region terrace and step edge. However, a satisfactory decomposition cannot be obtained unless the fourth component between the terrace and bulk, which was supposed from the contribution of Rh atoms in region underneath, is included. The relative binding energy shifts for the step edge, terrace and underneath components were attributed to their different coordination, i.e., less coordination results in larger shifts.

In Figure 1(c), the calculated CLSs versus CLSs decomposed from experiments are plotted. A perfect agreement between calculations and experiments may lead to a line crossing zero with a slope equal to one. Figure 1(c) shows the agreement is excellent, and the overall difference with respect to the measurements is less than 80 meV, irrespective to the different approximations used in CLS calculations (less than 50 meV for FS and TS approximations). The relative difference between IS approximation and approximations including the FS effect, such as the FS and GTS approximations, is less than 40 meV. These results indicate that for clean Rh(553) surface, the IS effects determined by the local coordination is dominating, while the FS effects from the electronic relaxation is modest. The dominating IS
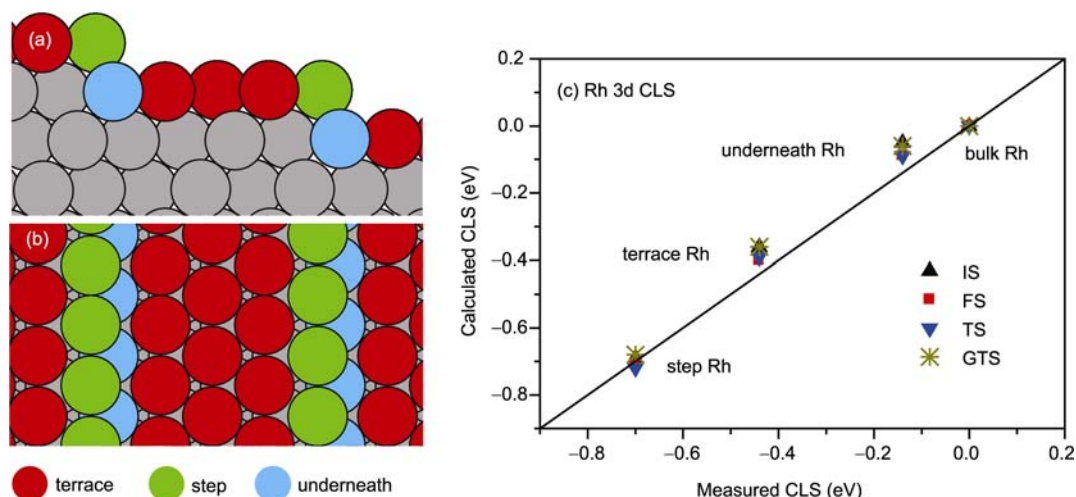
Figure 1   Side (a) and top (b) views of the vicinal Rh(553) surface with the three different coordination surface atoms, i.e., terrace, step edge and underneath atoms. (c) Measured [37] versus calculated Rh $3d_{5/2}$ CLS for Rh(553) terrace, step edge, underneath and bulk atoms. The results calculated by IS, FS, TS, and GTS theories are presented, respectively.

effects for clean transition metal surfaces were found in various transition metal surfaces [9]. The agreement between calculated and measured CLSs shows that the accuracy for the CLS calculations could be achieved in 50 meV for the transition metals considered here. The accuracy of the CLS calculations is crucial to interpret the measured XPS spectra.

In Table 1, we summarize typical CLS calculations including the FS effects on various transition metal surfaces available in refs. [9, 14–16, 20, 40]. The results agree with the experimental measurements, and the FS effects in these calculations are found to be small with the root of mean square deviation (RMSD) about 50 meV.

Table 1   Calculated and measured surface CLS in eV for surface metal atoms with respect to bulk atoms on various transition metal surfaces

TM	Surface	Calc.	Ref.	Exp.	Ref.
Mo 3d	(110)	−0.28	[9]	−0.33	[38]
Ru 3d	(0001)	−0.37 (0.12)	[15]	−0.38 (0.12)	[15]
Rh 3d	(111)	−0.42	[9]	−0.50	[9, 21]
		−0.50	[16]		
		−0.45	[17]		
		−0.46	[14]		
	(110)	−0.63	[9]	−0.64	[9]
	(100)	−0.64	[9]	−0.62	[21]
Pd 3d	(111)	−0.30	[9]	−0.28	[9]
	(110)	−0.44	[9]	−0.55	[9]
	(100)	−0.32	[9]	−0.44	[39]
Ag 3d	(111)	−0.14	[9]	<−0.1	[9]
	(100)	−0.10	[9]		
		−0.24	[40]		
Pt 4f	(111)	−0.40	[20]	−0.40	[41]
		−0.41	[22]	−0.42	[22]

4   NO adsorption on Pt(111) surface

To study the reactivity of TM surfaces, the detail knowledge of adsorption sites and structures is significant. Sensitivity of the CLS to the local environments demonstrated above provides a unique way to accomplish these goals. For molecular adsorption on TM surfaces, the chemical bonds are formed via the orbital hybridization between adsorbates and substrates, accompanied with certain charge transfer. The hybridization and charge transfer, which are dependent on sites and coordination, lead to the variation in core level binding energies for both adsorbates and substrates. As a result, both of them may have a shift in binding energies, which could be measured by XPS and calculated by DFT. The comparison between theoretical calculations and experiments could be used to identify the adsorption structures formed.

To illustrate this, we present a CLS calculation for NO adsorption on Pt(111) surface, which is a model system for industrial and environmental catalysis process of NO_x reduction. For NO adsorption on Pt(111) [20, 41], NO molecules prefer to adsorb at three-fold fcc hollow sites at low coverage and form a $p(2 \times 2)$-NO(fcc) structure at 0.25 monolayer (ML). At higher coverage, one-fold top site is occupied further and a $p(2 \times 2)$-2NO(fcc+top) structure at 0.50 ML is formed, in which three quarters surface Pt atoms coordinate with one fcc hollow site NO, while the remaining surface Pt atoms coordinate with one top site NO. Accordingly, there are no surface Pt atoms shared by any adsorbed NO. With the increase of NO coverage, the hcp sites are occupied becomes popular, and p(2 × 2)-3NO(fcc+top+ hcp) structure is formed at 0.75 ML. In this structure, there are three quarters surface Pt atoms shared by one fcc and one hcp hollow site NO.

The distinct coordinations between Pt and adsorbed NO
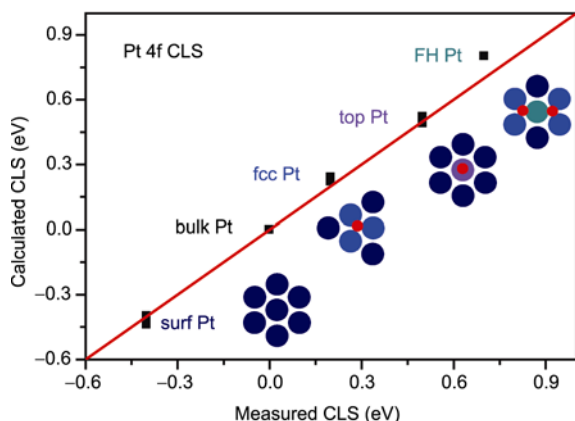
Figure 2 Calculated [20] versus measured [41] Pt $4f_{7/2}$ core level shifts of the first layer Pt atoms in different local environments for NO adsorption on Pt(111) surface. The shifts are calculated/measured with respect to the bulk Pt atoms.

Figure 3 (a) Pt $4f_{7/2}$ core-level spectra for O/Pt(111) and O/Pt(332) after saturation with oxygen at 310 K. In the decompositions, the dashed blue line is bulk, and the insets are CLSs from DFT calculations. (b), (c) Calculated equilibrium structures and average adsorption energy at (b) low and (c) high O coverage [23].

at different coverage can be seen from the evolution of corresponding Pt $4f_{7/2}$ CLS in both the experiment [41] and theory [20], as shown in Figure 2. For surface Pt atoms without bonding to any adsorbates (noted as surf. Pt), there is a negative shift with respect to the bulk Pt atoms due to the reduction of coordination, as found generally for clean TM surfaces (see Sec. 3). When Pt atoms are coordinated with one fcc NO (fcc Pt), a positive shift to higher binding energy is found because of the charge transfer from the substrates to adsorbed NO [20]. For surface Pt atoms coordinated with top site NO (top Pt), the same direction of charge transfer from the substrates to adsorbed NO occurs. Because charge transfer comes mainly from single-coordinated Pt atoms underneath (instead of contributing one-third for hollow site NO), a larger shift is observed. For NO adsorption at coverage 0.75 ML, in which one surface Pt atom shared by two hollow sites NO (FH Pt), the overall contributions from two NO molecules result in a significant large shift for corresponding Pt $4f_{7/2}$ level. Figure 2 shows the excellent agreement between calculated and measured CLSs.

5   Oxygen adsorption on vicinal Pt(332)

The interaction between oxygen and TM surfaces is fundamental important for various chemical processes. Besides its model characteristic for adsorbate-substrate interactions, it is crucial as the first step in oxidation of TM surfaces, and involves in various catalytic oxidation reactions, such as CO oxidation. Therefore, considerable efforts have been carried out concerning O adsorption or surface oxide on TM surfaces including XPS experiments and CLS calculations [14, 15, 23, 36, 40]. Valuable insights in terms of the oxygen-metal interaction in different chemical environments, such as preference of adsorption sites and coordination, have been obtained.

In Figure 3 (bottom panel), measured and calculated Pt
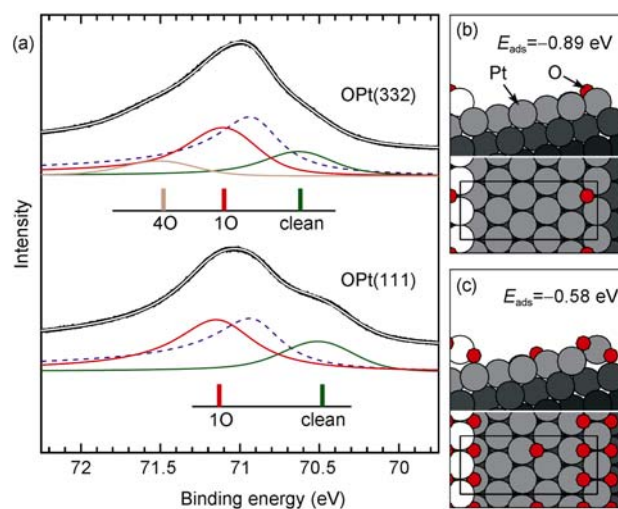
$4f_{7/2}$ core level shifts for oxygen dissociative adsorption on Pt (111) are plotted [23]. For oxygen dissociative adsorption on Pt (111) saturated at 310 K, a new peak (noted as 1O) was found with a higher binding energy than that of the peaks from the bulk and clean Pt atoms, which was supposed to be from the oxygen adsorption. CLS calculations confirmed this assignment, and showed that the shift was induced by fcc-hollow site oxygen, and the corresponding surface Pt atoms coordinated with one oxygen atom. When surface Pt atoms coordinates with more than one oxygen atom, large shift to higher energy are expected. This was found for oxygen adsorption on vicinal Pt (332) surface with six atom width (111) terrace separated by monoatomic (111) facet, as shown in Figure 3 (top panel). Because of its low coordination, the metal atoms along the step edge become highly active. A peak resolved at higher binding energy than oxygen coordinated terrace Pt (1O) was attributed to the edge Pt atoms coordinated with four oxygen (4O). DFT calculations show that the configuration is energetically favorable and the calculated Pt $4f_{7/2}$ CLSs agree well with the experimental results. It is noteworthy that the configuration identified at the Pt edge via the cooperation between XPS measurements and DFT calculations is one-dimensional PtO_2 oxide structure. The 1D oxide formed here acts as the nucleation site for the formation of the bulk oxide, which was also found in other transition metal surfaces [29, 42, 43].

6   CO adsorption on Pt and Rh surfaces

Due to the limitation of local and/or semi-local exchange-correlation functional used in DFT calculations, ground

state total energy calculations may not accurately describe the interaction between adsorbates and substrates, and in some case may even produce wrong results. One classic example is the famou*s CO puzzle p*roblem [44], in which CO prefers to adsorb at the one-fold top sites on Pt(111) and Rh(111) at low coverage as indicated by experiments, while DFT total energy calculations predict the three-fold hollow sites instead. The problem comes partly from the underestimation of CO's HUMO and LUMO gap in generalized-gradient approximation, which remains a subject under extensive investigations [45–47]. Theoretical difficulty in identification of CO adsorption sites could however be relieved by CLS calculations because of its independence on the functional [16, 17, 23].

Figure 4 shows the C 1s shift for CO adsorption on Pt(111) and Pt(332) surfaces experimentally and theoretically [23]. For CO/Pt(111), we found that the CLS from $c(4 \times 2)$-2CO (top + bridge) is in good agreement with experimental measurements, indicating CO adsorbs on the top site of Pt(111) surface first, despite the ambiguity in their ground state energies. For Pt (332), CO adsorbs first on the step edge due to its high reactivity, and then populates terrace top and bridge sites further. A new C 1s peak has not been found on Pt (111) at low CO exposures before the top and bridge C 1s peaks on the Pt (111) terrace occurs at higher coverage. DFT total energy calculations show that the energetic difference for CO adsorption between the top and bridge sites of the step is less than 30 meV, indicating both sites may be occupied. However, the calculated C 1s for these two sites is different. As shown in Figure 4(b), CO adsorption on the top site of the step can be concluded unambiguously from the comparison between calculated and measured CLS.
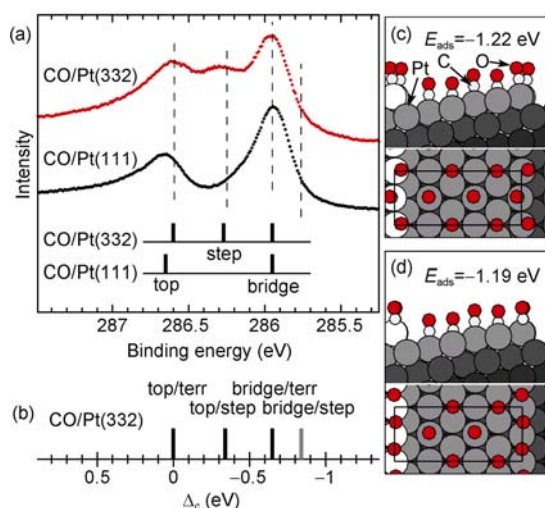
The sensitivity of C 1s shift of adsorbed CO molecules on coordination and local environments, revealed by XPS measurements and CLS calculations, could be used as a fingerprint for CO adsorption, diffusion and desorption on the TM surfaces. This is particularly useful for monitoring the reaction on solid-gas interface using fast *in situ* XPS [3]. In this context, we noticed that for NO adsorption on Pt(111), though the relative Pt $4f_{7/2}$ shifts of surface Pt atoms coordinated with various NO could be calculated accurately as shown above, the difference of calculated N and O 1s CLS with respect to the experiments is significantly large and falls in magnitude of 0.7 eV, which is far from the possible numerical error bar, as described in detail in ref. [20]. Compared with the CO molecule with empty $2\pi^*$ orbital, NO molecule has one electron occupied in the $2\pi^*$ orbital, whose interaction and relaxation with the core-hole may not be well described in the present DFT implementation and exchange-correlation functional. However, the exact reason for the large difference between theories and experiments remains unclear, and requires further theoretical studies.

7 $CH_x(x = 0–3)$ adsorption on Rh surfaces

Though chemical reactions could be monitored efficiently by fast *in situ* XPS, it remains a challenge to distinguish various spectra measured because there may be a number of intermediates with unknown peakes (in addition to reactants and products) during the reaction on the solid-gas interfaces. An interpretation of the measured XPS and corresponding reaction mechanism should be treated carefully. Additional characterizations and calculations in terms of their energetics and kinetics should to be performed.

We discuss this by presenting C 1s level shifts of $CH_x(x = 0–3)$ radicals with respect to carbon in CO on Rh(111) in Figure 5. These radicals are main intermediates in various industrial catalytic reactions such as methane acti vation,
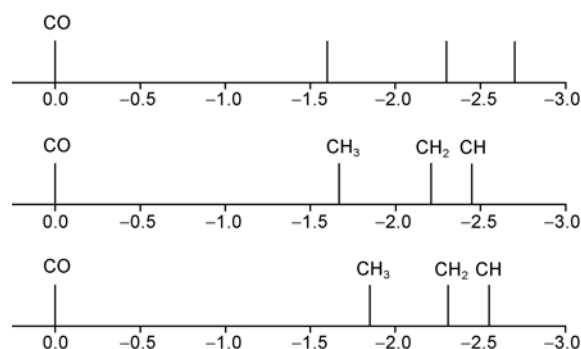

Figure 4   (a) C 1s spectra for CO adsorption on Pt(332) and Pt(111) showing an additional signal for step bonded CO; (b) calculated C 1s shifts for CO adsorption on Pt(332); (c), (d) structures and average adsorption energies per CO for CO/Pt(332). The dashed lines in (a) are based on the calculated shifts [23].

Figure 5   Calculated C 1s CLS for $CH_x(x = 0–3)$ radicals on clean (middle) and CO-modified (bottom) Rh(111) surface. The results for atomic carbon $(x = 0)$ is not indicated since it overlaps with CH radical. Measured C 1s spectrum from ethanol decomposition on Rh(111) from ref. [48] are given in top panel. The energy reference corresponds to top site CO on clean Rh(111) [19].

Fishcher-Tropsch synthesis, and methanol and ethanol conversion. A number of XPS measurements are available, and representative results derived from ethanol decomposition on Rh(111) are shown in the top panel of Figure 5, together with the calculated C 1s level shifts [19]. Though measured peaks could be correlated with various radicals including CH_2 from the comparison with the CLS calculations, the reaction barriers from DFT calculations indicate that the CH_2 radical is unstable, and should be therefore excluded. The corresponding peaks should come from other intermediates, instead of CH_2.

Our calculations show further that independence on Rh(111) and Rh(553) surfaces, C 1s in CH and atomic carbon is almost the same, though both of them have considerable shifts with respect to CO and CH_3 [25]. Therefore, it is impossible to distinguish the extent of the dehydrogenation of ethanol to either CH or atomic carbon on both surfaces from XPS measurements alone. DFT calculations show that the decomposition of CH radical on Rh(111) is endothermic, but becomes exothermic on Rh(553) due to the enhanced bonding of atomic carbon at the step edge, as shown in Figure 6. Further more, calculated reaction barrier for CH decomposition on Rh(553) is 0.37 eV lower than that of Rh(111) because of the favorable transition state formed at the step edge. These energetic and kinetic calculations show enhanced tendency of complete ethanol dehydrogenation on defected Rh surfaces, which is difficult to conclude from XPS measurements otherwise.

8   Summary and perspective

In this review, various examples are presented to illustrate the important role of the first-principles CLS calculations in deep understanding of chemical process in solid-gas interfaces. The accuracy and reliability of CLS calculations in comparison with the high resolution XPS measurements are
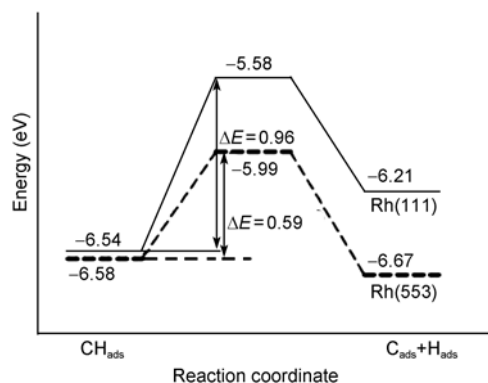
Figure 6   Potential energy surfaces (referenced to a CH radical in gas phase) for the initial state (left), the transition state (middle), and the final state (right) for the lowest energy dissociation paths on Rh(111) (solid lines) and Rh(553) (dashed lines). The activation energies (ΔE) for the two surfaces are indicated. All energies are in eV [25].

demonstrated. The interplay between CLS calculations and measurements, supplemented with additional energetic calculations and experimental characterizations, are illustrated to reveal the adsorption sites, structures, charge transfer and chemical reactions. Together with the advent of high-pressure and fast XPS benefiting from advanced light source for the chemical reactions in nanoparticle-gas interface under realistic conditions, the first-principle CLSs and DF calculations with the ability of describing the system with thousands of atoms would play an essential role in catalysis study.

From the theoretical point of view, we noticed that though valuable insights and progress have been obtained from the CLS calculations and cooperation of XPS measurements, further developments in XPS calculations are necessary. For instance, for XPS measurements, the specific core level binding energies as well as the intensity of the spectra are recorded. The information of intensity proportional to the coverage and its evolution during the reaction is one of the key issues to the reactivity and kinetic studies of the chemical process on solid-gas interfaces. However, explicit theoretical description of the spectrum intensity including the photon-electron scattering and its application remains. Accurate and efficient calculations of absolute core level binding energies, which would allow straightforward comparison with measurements instead of relative shifts, need to be improved for the extended solid-gas interfaces. Precise description of the excitation process, core-valence electron interaction and the electronic screening with better functional is required. CLS calculations for the chemical processes on metal oxide surfaces are less studied, and more efforts along this direction should be investigated.

Appendix

To illustrate the accuracy of the calculated absolute core-level binding energies using different approximations and DFT packages, we studied Rh 3d core-level binding energy of bulk and surface atoms of Rh(111) surface and their relative shift. The results are shown in Table A1. For both PAW and LAPW methods, the calculated absolute binding energies from IS approximation are far from the experimental results. The results are however improved for (G)TS approximation, and the agreement between FS approximation using LAPW method and experiments is better, and the difference in absolute binding energy is less than 0.5 eV. Compared with the calculated absolute binding energy, their

Table A1 Calculated absolute core-level binding energies and surface CLSs of Rh(111) using different DFT implementations and approximation methods. The experimental results in refs. [9, 21, 37, 49] are shown for comparison.

Method	State	BE (eV)		CLS (eV)
		bulk	surface	
USPP-FS	3d	–	–	−0.50
PAW-IS	3d	298.09	297.68	−0.41
PAW-TS	3d	313.04	312.61	−0.43
PAW-GTS	3d	313.15	312.65	−0.50
PAW-FS	3d	–	–	−0.45
LAPW-IS	$3d_{5/2}$	295.02	294.61	−0.41
LAPW-TS	$3d_{5/2}$	305.50	305.07	−0.43
LAPW-GTS	$3d_{5/2}$	305.55	305.08	−0.47
LAPW-FS	$3d_{5/2}$	307.58	307.13	−0.45
Exp.	$3d_{5/2}$	~307.2	~306.7	~−0.5

relative shifts are not sensitive to the method. In other words, IS approximation could describe surface Rh atoms CLS accurately, though (G)TS and FS approximation usually produce better results.

1   Spanjaard D, Guillot C, Desjonqueres MC, Treglia G, Lecante J. Surface core level spectroscopy of transition metals: A new tool for the determination of their surface structure. *Surf Sci Rep*, 1985, 5: 1–85

2   Hüfner S. *Photoelectron Spectroscopy: Principles and Applications*. Berlin: Springer, 2003

3   Baraldi A, Comelli G, Lizzit S, Kiskinova M, Paolucci G. Real-time X-ray photoelectron spectroscopy of surface reactions. *Surf Sci Rep*, 2003, 49: 169–224

4   Baraldi A. Structure and chemical reactivity of transition metal surfaces as probed by synchrotron radiation core level photoelectron spectroscopy. J Phys: Condens Matter, 2008, 093001

5   Tao F, Grass ME, Zhang YW, Butcher DR, Renzas JR, Liu Z, Chung JY, Mun BS, Salmeron M, Somorjai GA. Reaction-driven restructuring of Rh-Pd and Pt-Pd core-shell nanoparticles. *Science*, 2008, 322: 932–934

6   Feibelman PJ. First-principles calculational methods for surface-vacancy formation energies, heats of segregation, and surface core-level shifts. *Phys Rev B*, 1989, 39: 4872

7   Methfessel M, Hennig D, Scheffler M. *Ab initio* calculations of the initial-state and final-state effects on the surface core-level shift of transition-metals. *Surf Sci*, 1993, 287: 785–788

8   Alden M, Skriver HL, Johansson B. *Ab initio* surface core-level shifts and surface segregation energies. *Phys Rev Lett*, 1993, 71: 2449–2452

9   Andersen JN, Hennig D, Lundgren E, Methfessel M, Nyholm R, Scheffler M. Surface core-level shifts of some 4d-metal single-crystal surfaces–experiments and *ab-initio* calculations. *Phys Rev B*, 1994, 50: 17525–17533

10 Pasquarello A, Hybertsen MS, Car R. Si 2p core-level shifts at the Si(001)-SiO₂ interface–A first-principles study. *Phys Rev Lett*, 1995, 74: 1024–1027

11 Schmidt WG, Kackell P, Bechstedt F. 3d core-level shifts at Se/GaAs(110). *Surf Sci*, 1996, 358: 545–549

12 Cho JH, Kang MH, Terakura K. Si 2p core-level shifts at the As/Si(001) and Sb/Si(001) surfaces. *Phys Rev B*, 1997, 55: 15464–15466

13 Rignanese GM, Pasquarello A, Charlier JC, Gonze X, Car R. Nitro-

gen incorporation at Si(001)-SiO2 interfaces: Relation between N 1s core-level shifts and microscopic structure. *Phys Rev Lett*, 1997, 79: 5174–5177

14 Ganduglia-Pirovano MV, Scheffler M, Baraldi A, Lizzit S, Comelli G, Paolucci G, Rosei R. Oxygen-induced Rh 3d(5/2) surface core-level shifts on Rh(111). *Phys Rev B*, 2001, 63: 205415

15 Lizzit S, Baraldi A, Groso A, Reuter K, Ganduglia-Pirovano MV, Stampl C, Scheffler M, Stichler M, Keller C, Wurth W, Menzel D. Surface core-level shifts of clean and oxygen-covered Ru(0001). *Phys Rev B*, 2001, 63: 205419

16 Birgersson M, Almbladh CO, Borg M, Andersen JN. Density-functional theory applied to Rh(111) and CO/Rh(111) systems: Geometries, energies, and chemical shifts. *Phys Rev B*, 2003, 67: 045402

17 Köhler L, Kresse G. Density functional study of CO on Rh(111). *Phys Rev B*, 2004, 70: 165405

18 Ji W, Lu ZY, Gao H. Electron core-hole interaction and its induced ionic structural relaxation in molecular systems under X-ray irradiation. *Phys Rev Lett*, 2006, 97: 246101

19 Yang MM, Bao XH, Li WX. Density functional theory study of CH*x* (*x* = 1−3) adsorption on clean and CO precovered Rh(111) surfaces. *J Chem Phys*, 2007, 127: 024705

20 Zeng ZH, Da Silva JLF, Deng HQ, Li WX. Density functional theory study of the energetics, electronic structure, and core-level shifts of NO adsorption on the Pt(111) surface. *Phys Rev B*, 2009, 79: 205413

21 Baraldi A, Bianchettin L, Vesselli E, Gironcoli Sd, Lizzit S, Petaccia L, Zampieri G, Comelli G, Rosei R. Highly under-coordinated atoms at Rh surfaces: interplay of strain and coordination effects on core level shift. *New J Phys*, 2007, 9: 143

22 Bianchettin L, Baraldi A, de Gironcoli S, Vesselli E, Lizzit S, Petaccia L, Comelli G, Rosei R. Core level shifts of undercoordinated Pt atoms. *J Chem Phys*, 2008, 128: 114706

23 Wang JG, Li WX, Borg M, Gustafson J, Mikkelsen A, Pedersen TM, Lundgren E, Weissenrieder J, Klikovits J, Schmid M, Hammer B, Andersen JN. One-dimensional PtO₂ at Pt steps: Formation and reaction with CO. *Phys Rev Lett*, 2005, 95: 256102

24 Zhang W, Yang J, Luo Y, Monti S, Carravetta V. Quantum molecular dynamics study of water on TiO₂(110) surface. *J Chem Phys*, 2008, 129: 064703

25 Resta A, Gustafson J, Westerstrom R, Mikkelsen A, Lundgren E, Andersen JN, Yang MM, Ma XF, Bao XH, Li WX. Step enhanced dehydrogenation of ethanol on Rh. *Surf Sci*, 2008, 602: 3057–3068

26 Chong DP. Accurate calculation of core-electron binding energies by the density-functional method. *Chem Phys Lett*, 1995, 232: 486–490

27 Triguero L, Plashkevych O, Pettersson LGM, Agren H. Separate state vs. transition state Kohn-Sham calculations of X-ray photoelectron binding energies and chemical shifts. *J Electron Spectrosc Relat Phenom*, 1999, 104: 195–207

28 Olovsson W, Goansson C, Marten T, Abrikosov IA. Core-level shifts in complex metallic systems from first principle. *Physica Status Solidi (B)*, 2006, 243: 2447–2464

29 Lundgren E, Kresse G, Klein C, Borg M, Andersen JN, De Santis M, Gauthier Y, Konvicka C, Schmid M, Varga P. Two-dimensional oxide on Pd(111). *Phys Rev Lett*, 2002, 88: 246103

30 Todorova M, Lundgren E, Blum V, Mikkelsen A, Gray S, Gustafson J, Borg M, Rogal J, Reuter K, Andersen JN, Scheffler M. The Pd(100)-($\sqrt{5} \times \sqrt{5}$)R27°-O surface oxide revisited. *Surf Sci*, 2003, 541: 101–112

31 Weinert M, Watson RE. Core-level shifts in bulk alloys and surface adlayers. *Phys Rev B*, 1995, 51: 17168–17180

32 Slater JC. *Quantum Theory of Molecules and Solides*. New York: McGraw-Hill, 1974

33 Williams AR, deGroot RA, Sommers CB. Generalization of Slater's transition state concept. *J Chem Phys*, 1975, 63: 628–631

34 Janak JF. Proof that $\partial E/\partial n_i = \mathring{a}$ in density-functional theory. *Phys Rev B*, 1978, 18: 7165–7168

35 Marsman M, Kresse G. Relaxed core projector-augmented-wave method. *J Chem Phys*, 2006, 125: 104101

36 Reuter K, Scheffler M. Surface core-level shifts at an oxygen-rich Ru

surface: O/Ru(0001) vs. RuO$_2$(110). *Surf Sci*, 2001, 490: 20–28

37 Gustafson J, Borg M, Mikkelsen A, Gorovikov S, Lundgren E, Andersen JN. Identification of step atoms by high resolution core level spectroscopy. *Phys Rev Lett*, 2003, 91: 056102

38 Lundgren E, Johansson U, Nyholm R, Andersen JN. Surface core-level shift of the Mo(110) surface. *Phys Rev B*, 1993, 48: 5525–5529

39 Nyholm R, Qvarford M, Andersen JN, Sorensen SL, Wigren C. The surface core-level shift of the Pd(100) single-crystal surface. *J Phys: Condens Matter*, 1992, 4: 277–283

40 Gajdos M, Eichler A, Hafner J. *Ab initio* density functional study of O on the Ag(001) surface. *Surf Sci*, 2003, 531: 272–286

41 Zhu JF, Kinne M, Fuhrmann T, Denecke R, Steinrück HP. *In situ* high-resolution XPS studies on adsorption of NO on Pt(111). *Surf Sci*, 2003, 529: 384–396

42 Gustafson J, Mikkelsen A, Borg M, Lundgren E, Kohler L, Kresse G, Schmid M, Varga P, Yuhara J, Torrelles X, Quiros C, Andersen JN. Self-limited growth of a thin oxide layer on Rh(111). *Phys Rev Lett*, 2004, 92: 126102

43 Klikovits J, Schmid M, Merte LR, Varga P, Westerstrom R, Resta A, Andersen JN, Gustafson J, Mikkelsen A, Lundgren E, Mittendorfer F,

Kresse G. Step-orientation-dependent oxidation: From 1D to 2D oxides. *Phys Rev Lett*, 2008, 101: 266104

44 Feibelman PJ, Hammer B, Nørskov JK, Wagner F, Scheffler M, Stumpf R, Watwe R, Dumesic J. The CO/Pt(111) puzzle. *J Phys Chem B*, 2001, 105: 4018–4025

45 Wang Y, de Gironcoli S, Hush NS, Reimers JR. Successful a priori modeling of CO adsorption on pt(111) using periodic hybrid density functional theory. *J Am Chem Soc*, 2007, 129: 10402–10407

46 Hu QM, Reuter K, Scheffler M. Towards an exact treatment of exchange and correlation in materials: Application to the "CO adsorption puzzle" and other systems. *Phys Rev Lett*, 2007, 98: 176103

47 Alaei M, Akbarzadeh H, Gholizadeh H, de Gironcoli S. CO/Pt(111): GGA density functional study of site preference for adsorption. *Phys Rev B*, 2008, 77: 085414

48 Vesselli E, Baraldi A, Comelli G, Lizzit S, Rosei R. Ethanol decomposition: C-C cleavage selectivity on Rh(111). *ChemPhysChem*, 2004, 5: 1133–1140

49 Beutler A, Lundgren E, Nyholm R, Andersen JN, Setlik BJ, Heskett D. Coverage- and temperature-dependent site occupancy of carbon monoxide on Rh(111) studied by high-resolution core-level photoemission. *Surf Sci*, 1998, 396: 117–136